JBC Papers in Press. Published on February 17, 2005 as Manuscript M500997200

CALCIUM DYSREGULATION AND MEMBRANE DISRUPTION AS A UBIQUITOUS NEUROTOXIC MECHANISM OF SOLUBLE AMYLOID OLIGOMERS

Angelo Demuro[1+], Erene Mina[2+],Rakez Kayed[2], Saskia C. Milton[2], Ian Parker[1*], Charles G. Glabe[2*]

From the [1]Departments of Neurobiology and Behavior and [2] Department of Molecular Biology and Biochemistry, University of California Irvine, CA 92697, USA.

Running title: Membrane permeabilization by soluble amyloid oligomers.

[+]* These authors contributed equally to this work.

Address correspondence to: Dr. Charles Glabe, 3238 McGaugh Hall, Dept. of Molecular Biology and Biochemistry, UC Irvine, Irvine, CA 92697-3900, Tel. (949) 824-6081; Fax (949) 824-8551: cglabe@uci.edu

Increasing evidence suggests that amyloid peptides associated with a variety of degenerative diseases induce neurotoxicity in their intermediate oligomeric state, rather than as monomers or fibrils. To test this hypothesis and investigate the possible involvement of Ca^{2+} signaling disruptions in amyloid-induced cytotoxicity, we made homogeneous preparations of disease-related amyloids (Aß, Prion, IAPP, polyglutamine, and lysozyme) in various aggregation states and tested their actions on fluo-3-loaded SH-SY5Y cells. Application of oligomeric forms of all amyloids tested (0.6 - 6 μg ml^{-1}) rapidly (~ 5s) elevated intracellular Ca^{2+}, whereas equivalent amounts of monomers and fibrils did not. Ca^{2+} signals evoked by Aß42 oligomers persisted after depletion of intracellular Ca^{2+} stores, and small signals remained in Ca^{2+}-free medium; indicating contributions from both extracellular and intracellular Ca^{2+} sources. The increased membrane permeability to Ca^{2+} cannot be attributed to activation of endogenous Ca^{2+} channels, because responses were unaffected by the potent Ca^{2+}-channel blocker cobalt (20 μM). Instead, observations that Aß42 and other oligomers caused rapid cellular leakage of anionic fluorescent dyes point to a generalized increase in membrane permeability. The resulting unregulated flux of ions and molecules may provide a common mechanism for oligomer-mediated toxicity in many amyloidogenic diseases, with dysregulation of Ca^{2+} ions playing a crucial role owing to their strong trans-membrane concentration gradient and involvement in cell dysfunction and death.

Introduction

Alzheimer's disease (AD) is characterized by the appearance in the brain of plaques - containing extracellular deposits of amyloid ß-peptide (Aß) that result from altered proteolytic processing of amyloid precursor protein - together with intracellular neurofibrillary tangles containing misfolded tau (1). Brain regions with plaques and tangles exhibit reduced numbers of synapses, and neurites associated with plaques and tangles are often damaged, suggesting a pivotal role for Aß in the neuropathology of AD (2-5). Moreover, numerous other neurodegenerative disorders (including Huntington's, Parkinson's and prion diseases) are also associated with the formation and accumulation of amyloid fibrils in specific brain areas (6,7). These commonalities suggest a general mechanism of action for the more than 100 human amyloid-related diseases, whereby normally soluble peptides and proteins undergo aberrant folding (8).

Aggregation of Aß proceeds through several conformational states, including dimers, spherical oligomers composed of 10-24 monomers and strings of oligomers (protofibrils), before finally assuming an insoluble fibrillar conformation (9). The initial formulation of the "amyloid hypothesis" of AD specifically implicated fibrillar amyloid deposits (10). However, more recent evidence suggests that soluble oligomers may be the principal neurotoxic agent (11-15). Soluble Aß oligomers are found in the cerebrospinal fluid of AD patients (12): the soluble Aß content of human brain is better correlated with the severity of the disease than are the classical amyloid plaques containing insoluble Aß deposits (12,16): and fibril-free oligomers are toxic to cultured cells and neurons (11,15,17). Moreover, soluble oligomeric forms of several amyloids (including islet amyloid polypeptide (IAPP), α-synuclein, prion, and polyglutamine) are respectively implicated as the primary toxic species in type 2 diabetes mellitus, Parkinson's disease, spongiform encephalopathies, and Huntington's disease (6,15,18). This toxicity of amyloid oligomers appears to be intrinsically related to their aggregation state, because oligomeric forms of proteins and peptides that are not disease-related are equally toxic (14,19). Taken together, these findings support the notion of 'conformational disease' (20), whereby a common structural motif formed by otherwise unrelated amyloid oligomers leads to a common mechanism of pathogenesis (14,15). However, it remains to be established precisely which aggregation state is primarily responsible for the neurotoxicity; and difficulties in preparing highly homogeneous and stable populations of monomers, oligomeric intermediates and fibrils may account for observations of highly variable actions among different cells (21).

Questions also remain regarding the mechanism of amyloid toxicity. Growing evidence points to a disruption of intracellular Ca^{2+} homeostasis in AD and other amyloidogenic diseases (1,21,22), and elevated intracellular Ca^{2+} levels are known to trigger apoptosis and/or excessive phosphorylation of key proteins that ultimately lead to cell death (23-28). Pre-fibrillar amyloid aggregates have been shown to elevate cytosolic Ca^{2+} in neurons (19,21), but such actions have been proposed to be secondary to the generation of reactive oxygen species (1,29); to arise from activation of cell surface receptors coupled to Ca^{2+} influx (22,30-32); or to result from Ca^{2+} influx across the plasma membrane as a result of either cation-selective channels formed by Aß itself (21,33) or through a general disruption of lipid integrity (34).

To address these issues we prepared pure samples of monomeric, oligomeric and fibrillar forms of several disease-related amyloids and examined their respective actions on cytosolic Ca^{2+} levels in SH-SY5Y cells. We show that amyloid oligomers consistently produce rapid and dramatic elevations in $[Ca^{2+}]$, whereas equivalent concentrations of monomers or fibrils do not. The action of amyloid oligomers appears to involve a channel-independent disruption of the integrity of both plasma and intracellular membranes, and we propose that this may be a neurotoxic mechanism common to many amyloidogenic diseases.

Materials and Methods

Materials - Fluorescent dyes (fluo-3AM, calcein) and thapsigargin were from Molecular Probes (Eugene, OR). Ionomycin, cell culture media and other reagents were obtained from Sigma-Aldrich. Peptides were synthesized as described previously (35). Lyophilized peptides and proteins were resuspended in 50% acetonitrile in water and re-lyophilized.

Preparation of homogeneous populations of amyloid peptide monomers, oligomers and fibrils. - Soluble monomer and oligomers were prepared by dissolving 1.0 mg of peptide in 400 µl hexafluoroisopropanol (HFIP) for 10-20 min at room temperature. 100 µl of the resulting seedless solution was added to 900 µl double-distilled water in a siliconized Eppendorf tube. After 10-20 min incubation at room temperature, the samples were centrifuged for 15 min at 14,000 x G and the

supernatant fraction (pH 2.8-3.5) was transferred to a new siliconized tube and subjected to a gentle stream of N_2 for 5-10 min to evaporate the HFIP. The monomer solutions were used immediately after evaporation of HFIP. For soluble oligomers, the samples were then stirred at 500 rpm using a Teflon-coated micro stir bar for 24-48 h at 22ºC. Aliquots (10 µl) were taken at 6-12h intervals for observation by electron microscopy (EM) and size exclusion chromatography (SEC). For prion 106-126, the samples were heated at 65ºC for 30min before stirring. Poly Q was heated for 2h at 37ºC.

Fibrils were prepared as described above for oligomers, except they were stirred at room temperature for 6-9 days and sodium azide was added (0.02%). The final peptide concentration was 0.3 mg/ml. Fibril formation was monitored by thioflavin T fluorescence and UV light scattering. Once fibril formation was complete, the solutions were centrifuged at 14,000 x G for 20min, the fibril pellet was washed three times with double-distilled water, and then resuspended in the desired buffer. The morphology was verified by negative stain EM as previously reported (34).

Cell culture and dye loading - SH-SY5Y human neuroblastoma cells were maintained in Dulbecco`s modified Eagle`s medium (DMEM) (Gibco) supplemented with 10% fetal bovine serum, glutamine (4 mM), penicillin (200unit/ml), streptomycin (200 µg/ml), and sodium pyruvate (1 µM). Cells were maintained at 37°C in 5% CO_2 and the medium was replaced every 2 days. Cells (~10,000) were plated in 35mm glass-bottom culture dishes (MatTek Corporation) and grown overnight. Loading with the Ca^{2+} indicator fluo-3 was accomplished by incubating with fluo-3-AM (7 µM in Hank's Balanced Salt Solution) for 30 min at room temperature, washing 3 times with HBSS and maintaining at 37°C for 20 min to ensure complete hydrolysis. A similar loading protocol was utilized to load cells with calcein, by incubating with 7 µM calcein-AM.

Fluorescence Imaging - The imaging system consisted of an inverted microscope (Olympus IX 71) equipped with a Leitz 16X objective. Fluorescence excitation was by a 488 nm argon ion laser, and emitted fluorescence (λ>510 nm) was imaged by a cooled c.c.d. camera (Cascade 650, Roper Scientific). Time-lapse images (1 frame s^{-1}) were captured using the MetaMorph software package (Universal Imaging, Westchester, PA), and fluorescence intensities were measured from regions of interest centered on individual cells. Signals are expressed as a pseudo ratio ($\Delta F/F$) of the change in fluorescence (ΔF) divided by the resting fluorescence before treatment (F). A small proportion (9 %) of cells failed to load with fluo-3, having low initial fluorescence and failing to respond to ionomycin. These were excluded from analysis.

Amyloids were applied by pipetting a fixed aliquot (70 µl) of a diluted stock solution into the recording chamber (1 ml volume) directly above the microscope objective. To estimate the resulting concentration experienced by the cells under observation we pipetted the same volume of a fluorescent dye (calcein) into the chamber, and measured the resulting fluorescence in the vicinity of the cells relative to that of the initial, undiluted solution of dye. This calibration yielded a dilution factor of about 5, which was assumed in calculating the effective concentrations of amyloids.

To avoid complications from differences in molecular weights between monomers, oligomers and fibrils, we express these concentrations in units of µg ml^{-1}. As a rough guide, a concentration of 0.6 µg ml^{-1} Aß42 corresponds to 200 nM monomer, and approximately 7 nM oligomer and 70 pM fibrils.

RESULTS

Aß42 oligomers, but not monomers or fibrils, increase intracellular free Ca^2 - Homogeneous populations of monomeric, oligomeric and fibrillar Aß were prepared as described above and characterized by size exclusion chromatography and electron

microscopy. The oligomeric preparation had an approximate molecular mass of 90 kDa, contained very little material of lower molecular mass, and was comprised of spherical vesicles with diameters of 2-5 nm (Figure 1). The monomeric preparation contained no detectable oligomeric aggregates as analyzed by size exclusion chromatography (Figure 1). The morphology of the fibrillar preparations was as previously published (34).

The actions of homogeneous monomeric, oligomeric and fibrillar preparations of soluble Aß42 amyloid were examined by adding aliquots of the samples to fluo-3 loaded SH-SY5Y cells (Figure. 2). Figure 2A illustrates images and corresponding Ca^{2+}-dependent fluorescence measurements in a representative cell. Applications of monomers or fibrils at final concentrations of 6 μg ml^{-1} evoked no detectable change in fluorescence, whereas subsequent application of the same amount of oligomer evoked large and rapid (~ 5 s) increases in Ca^{2+}-dependent fluorescence. Similar results were obtained in > 200 cells examined. For example, Figure 2B shows mean fluorescence signals from 22 cells, where Aß42 oligomers evoked a fluo-3 signal with a peak increase of $\Delta F/F = 3.3 \pm 0.5$ (SEM).

The fact that monomeric and fibrillar samples were inactive rules out the possibility that the increase in Ca^{2+} was due to trace contaminants in the solvent, because the solvent remained the same over the time of incubation for the conversion of monomer to oligomer and then ultimately to fibrils. Solvent controls in the absence of peptide had no effect on Ca^{2+} levels (data not shown).

Actions of other disease-related amyloids - To explore the possibility of a common neurotoxic mechanism among amyloidogenic diseases, we selected five disease-related amyloid peptides (Aß42, prion, IAPP, polyglutamine, and lysozyme) and tested the effects of purified monomers, oligomers and fibrils of each of these amyloids on cytosolic Ca^{2+}. Figure 3A illustrates representative fluorescence records obtained with IAPP at a concentration of 6 μg ml^{-1}. Applications of IAPP monomers and fibrils evoked no detectable Ca^{2+} signals, even though the same cells showed large increases in fluorescence when subsequently challenged with the Ca^{2+} ionophore ionomycin (Figure 3A, traces a, b). In marked contrast, equivalent amounts of purified IAPP oligomers produced a large fluorescence signal (Figure 3A, trace c), closely resembling the response evoked by Aß42 oligomers.

Mean results obtained with all five amyloids are summarized in Figure 3B. In each case the oligomeric forms evoked large increases in intracellular [Ca^{2+}] (respective peak $\Delta F/F$ values Aß42 = 3.3 ±0.08; prion = 2.18 ±0.1; IAPP = 2.45 ±0.19; polyglutamine = 3.58 ±0.07; lysozyme = 2.77 ±0.1), whereas monomers and fibrils failed to produce any appreciable signal. Among a total of 1320 cells analyzed, 1280 showed Ca^{2+} responses to oligomers, whereas we never observed appreciable ($\Delta F/F > 0.4$) fluorescence increases with monomers or fibrils.

Concentration-dependence of oligomer action **-** We next examined the concentration-dependence of the Ca^{2+} signals on oligomer concentration, using IAPP and Aß42 as representative amyloids. The protocol is illustrated in Figure 4A, and involved sequential additions of oligomer to the imaging chamber, resulting in stepwise increases in concentration. Concentrations of IAPP oligomer as low as 0.6 μg/ml (corresponding to 7.5 nM assuming a molecular mass of 80 kDa) already evoked a detectable fluorescence increase, and 12 μg/ml (about 150 nM) produced a maximal response, as assessed by the failure of ionomycin to cause any further increase in fluorescence (not shown). Figure 4B shows mean measurements of relative fluorescence signals evoked by increasing concentrations of Aß42 and IAPP oligomers. Both amyloids showed similar concentration-response relationships, with half-maximal responses at respective concentrations of 2.7 and 3.5 μg/ml. These values may, however,

underestimate the true EC_{50} of the oligomers if the indicator dye were saturated at higher concentrations.

Elevation of cytosolic free Ca^{2+} from Aß42 oligomers involves both intra- and extracellular sources - To discriminate whether the increase in cytosolic Ca^{2+} concentration evoked by amyloid oligomers arises from influx of extracellular Ca^{2+} across the plasma membrane or from Ca^{2+} liberated from intracellular stores, we reduced the free extracellular Ca^{2+} concentration to very low levels by bathing cells for 20 min in a Ca^{2+}-free medium that included 5 mM Mg^{2+} and 10 mM EGTA. Application of Aß42 oligomers (6 μg/ml) then evoked only a small, slowly rising fluorescence signal, which reached a peak amplitude of about 30% of that in Ca^{2+}-containing medium (Figure 5A). Thus, the large, immediate Ca^{2+} increase induced by oligomers appears to result from influx of extracellular Ca^{2+}, whereas the remaining small, slow component may arise from intracellular Ca^{2+} liberation.

To confirm the latter interpretation we then depleted the endoplasmic reticulum Ca^{2+} stores of cells bathed in normal [Ca^{2+}] medium by applying thapsigargin, a specific SERCA pump inhibitor. Thapsigargin evoked a small rise in the Ca^{2+} signal, consistent with leakage of Ca^{2+} from intracellular stores into the cytosol, but subsequent application of Aß42 oligomers produced a large, rapid increase, similar to that observed in control cells without thapsigargin treatment (Figure 5B).

We examined the possibility that amyloidogenic peptides may induce Ca^{2+} influx via endogenous Ca^{2+}-permeable plasma membrane ion channels (30,31) by applying Aß42 oligomers (6 μg/ml) in the presence of 20 μM cobalt, a non-specific Ca^{2+} channel blocker (Figure 5A). Fluorescence signals were of almost identical amplitude in the presence (black trace) and absence (gray trace) of cobalt, suggesting that Ca^{2+} entry through cobalt-sensitive plasma membrane channels does not contribute significantly to the oligomer-induced rise in cytosolic [Ca^{2+}]. Similarly, the AMPA receptor antagonist, CNQX (40 μM) failed to block Ca^{2+} entry (22): the mean fluorescence signal evoked by Aß42 oligomers (6 μg/ml) in the presence of CNQX ($\Delta F/F = 1.80 \pm 0.24$, SEM, n = 32) was similar to that in parallel control experiments ($\Delta F/F = 1.70 + 0.27$, n = 47).

Decay of the oligomer-induced fluorescence signal is due to dye leakage - As evident in Figures 2-5, high concentrations of Aß42 consistently evoked a transient fluorescence signal that decayed over tens of seconds or a few minutes even in the continued presence of amyloid oligomers. The experiments illustrated in Figure. 6 indicate that this decay does not reflect a fall in cytosolic free [Ca^{2+}], but rather that Aß42 induces a general increase in membrane permeability, thereby allowing leakage of dye into the extracellular medium.

Firstly, ionomycin failed to induce any rise in fluorescence when applied late in the decay phase of a response to Aß42 oligomers (Fig. 6A). Secondly, Aß42 oligomers evoked an almost complete loss of fluorescence from cells loaded with the Ca^{2+}- and pH-insensitive dye calcein (Figure. 6B). Finally, measurements of fluorescence in the extracellular fluid adjacent to calcein-loaded cells showed a transient rise synchronous with the abrupt drop in intracellular fluorescence evoked by oligomers (Figure. 6C). Fluo-3 fluorescence also appears in the medium coincident with its loss from the cells (data not shown). Interestingly, ionomycin caused no change in fluorescence of intracellular calcein (Figure. 6B), indicating that the increase in dye permeability induced by Aß42 oligomers results from a direct action on the cell membrane and is not secondary to a rise in intracellular [Ca^{2+}].

The effect of Aß42 to induce a leakage of anionic dyes was shared by other soluble oligomers. Loss of fluo-3 fluorescence like that illustrated in Fig. 6A was consistently observed with equivalent concentrations of prion peptide (n = 51 cells), IAPP (n = 69), polyglutamine (n = 44) and lysozyme (n = 102).

DISCUSSION

We show that extracellular applications of spherical oligomeric forms of

Aß42 and several other disease-related amyloidogenic proteins and peptides cause an immediate and large increase in cytosolic free [Ca^{2+}], whereas equivalent amounts of monomeric and fibrillar forms are without any detectable effect. These results, obtained with highly homogeneous preparations, support a growing body of evidence that the aggregation state of these amyloids, rather than their specific amino acid sequences, is the key factor determining their toxicity (14,15).

Several mechanisms have been proposed to account for the Ca^{2+} mobilizing actions of amyloids in their oligomeric and fibrillar aggregation states. These include a direct interaction with membrane components to destabilize the membrane structure (36-39); insertion into the membrane to form a cation-conducting pore (21,34,40-44); activation of cell surface receptors coupled to Ca^{2+} influx (30-32); and oxidative stress leading to dysregulation of mitochondrial Ca^{2+} homeostasis (1). Among these possibilities, our data favor the hypothesis of a generalized increase in membrane permeability induced specifically by spherical amyloid oligomers. The rise in cytosolic Ca^{2+} following addition of oligomers is so rapid (one or a few seconds) as to preclude it being a secondary effect resulting from metabolic impairment and reduced Ca^{2+} pumping or sequestration. Moreover, several observations argue against Ca^{2+} influx through either endogenous Ca^{2+} membrane channels, or through cation-selective channels formed by the amyloid proteins themselves. Firstly, Ca^{2+} signals were not reduced in the presence of 20 μM cobalt, a non-specific blocker of many Ca^{2+}-permeable channels (45), or after applying CNQX to block Ca^{2+}-permeable AMPA receptor/channels (22). Secondly, all the amyloid oligomers we tested induced a rapid leakage of fluorescent dyes from cells loaded with fluo-3 and calcein, in agreement with a reports showing release of dye from phospholipid vesicles (46,47). Both fluo-3 and calcein are polyanionic molecules that are not expected to permeate through cation-selective channels, and have molecular masses (respectively, 854 and 622 Da) greater than the size cut-off for most ion channels. Finally, we note that although the major part of the oligomer-induced Ca^{2+} elevation arose through entry of extracellular Ca^{2+} ions, a remaining component in Ca^{2+}-free medium points to liberation of Ca^{2+} from intracellular stores. We thus propose that amyloid oligomers exert an immediate action by increasing the permeability of the plasma membrane, and subsequently penetrate into cells, as previously proposed (19), where they similarly disrupt intracellular membranes to cause leakage of sequestered Ca^{2+}.

Given the non-specific increase in membrane permeability, it is probable that amyloid oligomers will disrupt the intracellular homeostasis of many ions and other cellular constituents in addition to Ca^{2+}. Their actions on Ca^{2+} signaling are, however, likely to mediate the major cytotoxic effects. Firstly, resting cytosolic free [Ca^{2+}] is normally maintained at very low levels despite enormous trans-membrane concentration gradients, so that even a small increase in Ca^{2+} permeability will result in a proportionately large elevation of cytosolic [Ca^{2+}]. In agreement, Ca^{2+} signals were evident at concentrations of oligomers that failed to induce any detectable dye leakage. Secondly, Ca^{2+} dyshomeostasis is definitively implicated in both necrotic and apoptotic cell death (23), and amyloid-induced Ca^{2+} changes are directly correlated with cell viability (19). Nevertheless, it remains possible that perturbations of other ions and molecules may contribute to the long term pathogenesis of amyloid diseases. An intriguing possibility in neurological diseases is that an enhanced plasma membrane ion conductance may cause a sustained depolarization and increased electrical excitability, leading to excitotoxic injury.

We observed half-maximal Ca^{2+} elevations with Aß and IAPP oligomers at concentrations of about 3 μg ml^{-1}, and consistent signals remained at 0.6 μg ml^{-1} (equivalent to about 7 nM). These concentrations are considerably lower than used in most previous studies, and the Ca^{2+} signals were immediate, rather than rising over several minutes or after long latencies (19,21), possibly reflecting a higher purity of the active

amyloid oligomers in our preparations. In comparison to the levels of soluble Aß measured in the brain of AD patients, however, the oligomer concentrations required to evoke immediate Ca^{2+} signals are 100 - 1000 times greater (12). The obvious difference is that whereas high concentrations of amyloid oligomers evoke an acute and dramatic increase in cytosolic free [Ca^{2+}], the pathophysiology of AD likely involves the cumulative effects of a much smaller but chronic disruption of Ca^{2+} homeostasis over several years. Moreover, the Ca^{2+} mobilizing action of Aß oligomers may be only one mechanism contributing toward Ca^{2+} signaling disruptions as a common pathway for neurotoxicity in AD. Early-onset AD is associated with mutations in the *presenilin* (*PS*) genes, and neurons from knock-in mice expressing an AD-linked mutation in *PS1* display greatly exaggerated release of Ca^{2+} from intracellular stores (48).

REFERENCES

1. Mattson, M. P. (2004) *Nature* **430**, 631-639
2. Kosik, K. S. (1992) *Science* **256**, 780-783
3. Selkoe, D. J. (1991) *Sci. Am.* **265**, 68-71, 74-66, 78
4. Tanzi, R. E., Gusella, J. F., Watkins, P. C., Bruns, G. A., St George-Hyslop, P., Van Keuren, M. L., Patterson, D., Pagan, S., Kurnit, D. M., and Neve, R. L. (1987) *Science.* **235**, 880-884
5. Haass, C., and Selkoe, D. J. (1993) *Cell* **75**, 1039-1042
6. Lashuel, H. A., Hartley, D. M., Balakhaneh, D., Aggarwal, A., Teichberg, S., and Callaway, D. J. (2002) *J Biol Chem* **277**, 42881-42890.
7. Stefani, M., and Dobson, C. M. (2003) *J Mol Med* **81**, 678-699
8. Dobson, C. M. (2004) *Science* **304**, 1259-1262
9. Glabe, C. G. (2004) *Trends Biochem Sci* **29**, 542-547
10. Hardy, J. A., and Higgins, G. A. (1992) *Science* **256**, 184-185
11. Lambert, M. P., Barlow, A. K., Chromy, B. A., Edwards, C., Freed, R., Liosatos, M., Morgan, T. E., Rozovsky, I., Trommer, B., Viola, K. L., Wals, P., Zhang, C., Finch, C. E., Krafft, G. A., and Klein, W. L. (1998) *Proceedings of the National Academy of Sciences of the United States of America* **95**, 6448-6453
12. Lue, L. F., Kuo, Y. M., Roher, A. E., Brachova, L., Shen, Y., Sue, L., Beach, T., Kurth, J. H., Rydel, R. E., and Rogers, J. (1999) *American Journal of Pathology* **155**, 853-862
13. Hardy, J., and Selkoe, D. J. (2002) *Science* **297**, 353-356.
14. Bucciantini, M., Giannoni, E., Chiti, F., Baroni, F., Formigli, L., Zurdo, J., Taddei, N., Ramponi, G., Dobson, C. M., and Stefani, M. (2002) *Nature* **416**, 507-511.
15. Kayed, R., Head, E., Thompson, J. L., McIntire, T. M., Milton, S. C., Cotman, C. W., and Glabe, C. G. (2003) *Science* **300**, 486-489
16. Naslund, J., Haroutunian, V., Mohs, R., Davis, K. L., Davies, P., Greengard, P., and Buxbaum, J. D. (2000) *Jama* **283**, 1571-1577.
17. Dahlgren, K. N., Manelli, A. M., Stine, W. B., Jr., Baker, L. K., Krafft, G. A., and LaDu, M. J. (2002) *J Biol Chem* **277**, 32046-32053.
18. Caughey, B., and Lansbury, P. T. (2003) *Annu Rev Neurosci* **26**, 267-298

19. Bucciantini, M., Calloni, G., Chiti, F., Formigli, L., Nosi, D., Dobson, C. M., and Stefani, M. (2004) *J Biol Chem* **279**, 31374-31382
20. Carrell, R. W., and Lomas, D. A. (1997) *Lancet* **350**, 134-138
21. Kawahara, M., Kuroda, Y., Arispe, N., and Rojas, E. (2000) *Journal of Biological Chemistry* **275**, 14077-14083
22. Blanchard, B. J., Chen, A., Rozeboom, L. M., Stafford, K. A., Weigele, P., and Ingram, V. M. (2004) *Proc Natl Acad Sci U S A* **101**, 14326-14332
23. Berridge, M. J., Bootman, M. D., and Lipp, P. (1998) *Nature* **395**, 645-648
24. Pierrot, N., Ghisdal, P., Caumont, A. S., and Octave, J. N. (2004) *J Neurochem* **88**, 1140-1150
25. Tucker, H. M., Rydel, R. E., Wright, S., and Estus, S. (1998) *Journal of Neurochemistry* **71**, 506-516
26. Mattson, M. P., and Rydel, R. E. (1992) *Neurobiol. Aging.* **13**, 617-621
27. Li, Y. P., Bushnell, A. F., Lee, C. M., Perlmutter, L. S., and Wong, S. K. (1996) *Brain Res* **738**, 196-204
28. LaFerla, F. M. (2002) *Nat Rev Neurosci* **3**, 862-872
29. Schubert, D., Behl, C., Lesley, R., Brack, A., Dargusch, R., Sagara, Y., and Kimura, H. (1995) *Proc Natl Acad Sci U S A* **92**, 1989-1993
30. Guo, Q., Furukawa, K., Sopher, B. L., Pham, D. G., Xie, J., Robinson, N., Martin, G. M., and Mattson, M. P. (1996) *Neuroreport* **8**, 379-383
31. Mattson, M. P., and Chan, S. L. (2003) *Nat Cell Biol* **5**, 1041-1043
32. Blanchard, B. J., Chen, A., Rozeboom, L. M., Stafford, K. A., Weigele, P., and Ingram, V. M. (2004) *Proc Natl Acad Sci U S A*
33. Kagan, B. L., Hirakura, Y., Azimov, R., Azimova, R., and Lin, M. C. (2002) *Peptides* **23**, 1311-1315.
34. Kayed, R., Sokolov, Y., Edmonds, B., MacIntire, T. M., Milton, S. C., Hall, J. E., and Glabe, C. G. (2004) *J Biol Chem*
35. Burdick, D., Soreghan, B., Kwon, M., Kosmoski, J., Knauer, M., Henschen, A., Yates, J., Cotman, C., and Glabe, C. (1992) *J Biol Chem* **267**, 546-554
36. Muller, W. E., Koch, S., Eckert, A., Hartmann, H., and Scheuer, K. (1995) *Brain Res* **674**, 133-136
37. Avdulov, N. A., Chochina, S. V., Igbavboa, U., Warden, C. S., Vassiliev, A. V., and Wood, W. G. (1997) *J Neurochem* **69**, 1746-1752
38. Mason, R. P., Trumbore, M. W., and Pettegrew, J. W. (1996) *Ann. N. Y. Acad. Sci.* **777**, 368-373
39. Green, J. D., Kreplak, L., Goldsbury, C., Li Blatter, X., Stolz, M., Cooper, G. S., Seelig, A., Kistler, J., and Aebi, U. (2004) *J Mol Biol* **342**, 877-887
40. Arispe, N., Rojas, E., and Pollard, H. B. (1993) *Proc. Natl. Acad. Sci. U. S. A.* **90**, 567-571
41. Arispe, N. (2004) *J Membr Biol* **197**, 33-48
42. Lin, M. A., and Kagan, B. L. (2002) *Peptides* **23**, 1215-1228.
43. Kawahara, M., Arispe, N., Kuroda, Y., and Rojas, E. (1997) *Biophys J* **73**, 67-75
44. Hirakura, Y., Lin, M. C., and Kagan, B. L. (1999) *Journal of Neuroscience Research* **57**, 458-466
45. Hille, B. (2001) *Ion channels of excitable membranes.*, Sinauer, Sunderland, MA

46. Anguiano, M., Nowak, R. J., and Lansbury, P. T., Jr. (2002) *Biochemistry* **41**, 11338-11343.
47. Relini, A., Torrassa, S., Rolandi, R., Gliozzi, A., Rosano, C., Canale, C., Bolognesi, M., Plakoutsi, G., Bucciantini, M., Chiti, F., and Stefani, M. (2004) *J Mol Biol* **338**, 943-957
48. Stutzmann, G. E., Caccamo, A., LaFerla, F. M., and Parker, I. (2004) *J Neurosci* **24**, 508-513

ACKNOWLEDGEMENTS

This work was supported by grants GM48071 (to I.P.) and AG00538, NS31230 and a grant from the Larry L. Hillblom Foundation (to C.G.). Conflict of Interest: Charles Glabe and Rakez Kayed are consultants for Kinexis, Inc.

FIGURE LEGENDS

Fig. 1. Size exclusion chromatography and morphology of pure Aß42 oligomers. The homogeneity and purity of Aß42 monomer and oligomer preparations were analyzed using size exclusion chromatography. Oligomers eluted between 12 and 15 min, which corresponds to an approximate molecular weight of 90,000 Da. Monomers eluted between 22 and 25 min. Inset image shows typical spherical oligomers (~3-5nm in diameter) formed after 48h of stirring.

Fig. 2. Aß42 oligomers, but not monomers or fibrils, elevate intracellular free [Ca^{2+}]. (A) Time course of Ca^{2+}-dependent fluorescence recorded from a single fluo-3-loaded SH-SY5Y cell in response to sequential application of monomers, fibrils, and oligomers of Aß42 (each at a final concentration of 6 μg/ml). Inset images of the cell were captured at the times indicated during the trace, and are depicted on a pseudocolor scale with 'warmer' colors on a rainbow scale corresponding to higher fluorescence. (B) Trace shows the average responses from 22 cells, evoked using the same protocol. Error bars indicate ± 1 S.E.M.

Fig. 3. Ca^{2+} elevations induced by other amyloids depend upon their aggregation state. (A) Fluorescence records illustrating typical responses to applications of 6 μg/ml of Aß42 monomer (a), fibrils (b), and oligomers (c) Each trace was obtained from a different cell. No responses were observed to monomers or fibrils, even though the same cells gave large signals when subsequently challenged with ionomycin (6 μM). (B) Pooled data showing mean fluorescence signals (± S.E.M.) from 40 - 200 cells evoked by Aß42, prion, IAPP, polyQ, and lysozyme; each at a final concentration of 6 μg ml^{-1}. Measurements were obtained from records like those in (A). For each amyloid, the histogram bars show responses evoked by monomers, fibrils and oligomers.

Fig. 4. Dose-dependence of Aß42 and IAPP oligomers. (A) Trace show Ca^{2+}-dependent fluorescence signals averaged from 26 cells in response to successive additions of IAPP oligomers, resulting in stepwise concentration increases to final levels of 0.6, 2.4, 6 and 12 μg/ml. Inset images show pseudocolor representations of a single cell, captured at the times indicated by the trace. (B) Mean peak fluorescence signals evoked by different concentrations of Aß (red bars) and IAPP (blue bars) oligomers. Data are from 78 cells for IAPP and 85 for Aß42, and are expressed as a percentage of the maximal response evoked by 12 μg ml^{-1} oligomer.

Fig. 5. Aß42 oligomer-induced rise in cytosolic [Ca^{2+}] involves Ca^{2+} ions from both extracellular and intracellular sources. (A) Ca^{2+} signals were reduced, but not abolished, when Aß42 oligomers (6 μg ml^{-1}) were applied to cells bathed in Ca^{2+}-free medium. The trace shows the mean fluorescence (± 1 S.E.M.) from 31 cells. (B) Depletion of ER Ca^{2+} stores does not abolish oligomer-induced Ca^{2+} signals in cells bathed in normal (1.8 mM Ca^{2+}) medium. Following pretreatment with 5μM thapsigargin, a specific blocker of SERCA Ca^{2+} pumps, applications of 6 μg ml^{-1} Aß42 oligomers induced a large, rapid rise in fluorescence with an amplitude ($\Delta F/F$ = 0.7) similar to that obtained in the absence of thapsigargin ($\Delta F/F$ = 0.5). Trace shows mean ± 1 S.E.M. of results in 38 cells. (C) Ca^{2+} signals evoked by Aβ42 oligomers are not reduced by cobalt, a nonspecific Ca^{2+} channel blocker. Cells were pretreated with 20μM cobalt for 10 min. Subsequent application of 6 μg/ml of Aß42 oligomers evoked a mean Ca^{2+}-dependent fluorescence signal (black trace) of similar amplitude and kinetics to that in the absence of Cobalt (gray trace). Data with cobalt were obtained from 27 cells. Control data (gray trace) are reproduced from Figure. 3A, trace c.

Fig. 6. Aß42 oligomers cause a general increase of membrane permeability. (A) The decline of fluo-3 fluorescence following high doses of Aß42 oligomers results from dye leakage, not a decline of cytosolic [Ca^{2+}]. Trace shows fluo-3 fluorescence from a single cell challenged with the Ca^{2+} ionophore ionomycin following decay of the fluorescence signal evoked by Aß42 oligomers. (B) Aß42 oligomers induce cellular leakage of the Ca^{2+}-insensitive dye calcein. Trace shows mean fluorescence monitored from the soma of cells loaded with calcein by incubation with AM ester. Application of ionomycin failed to cause any change in fluorescence, whereas subsequent addition of 6 μg ml^{-1} of Aß42 oligomers resulted in almost complete loss of cellular fluorescence. The record is a mean (± 1 S.E.M.) from 57 cells, and the inset images show representative fluorescence of a group of cells captured at the times marked on the trace. (C) Loss of intracellular calcein is accompanied by a rise in extracellular fluorescence. Traces show representative examples from three cells, illustrated (before addition of oligomer) in the panels at the right. In each case fluorescence was monitored from the cell soma (black traces) and from regions of interest positioned just outside the cells (red traces: regions marked by white outlines on the images).

Figure 1.

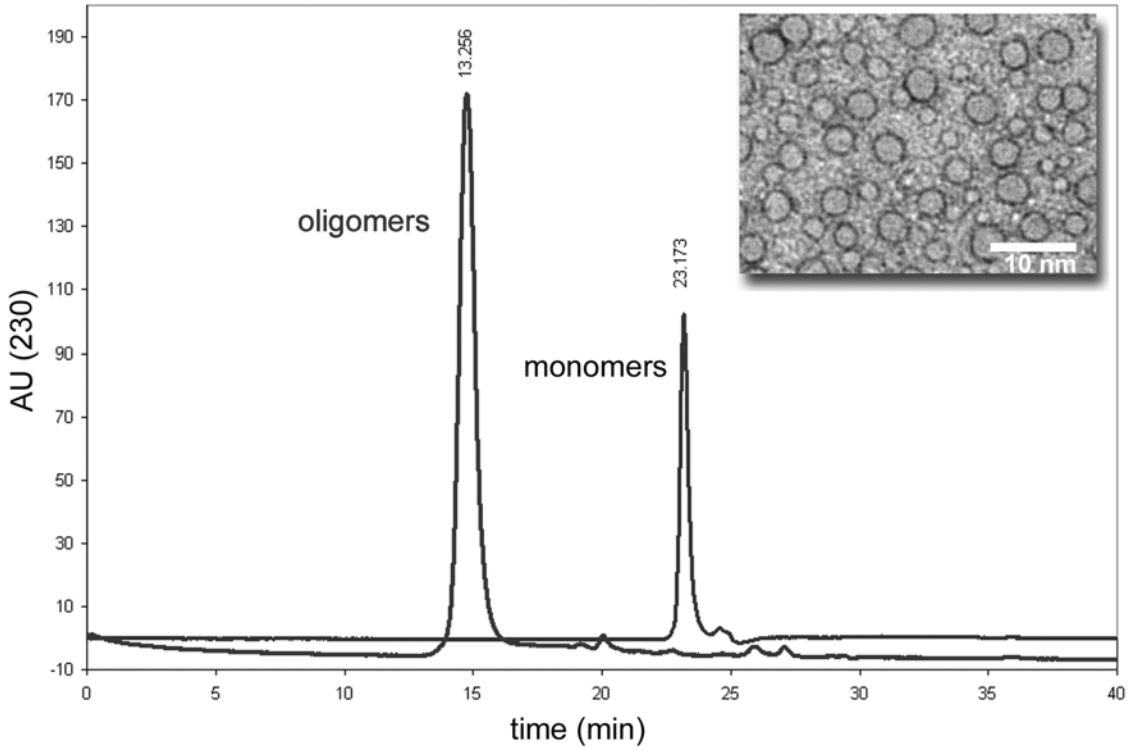
13.256
oligomers
23.173
monomers
10 nm
AU (230)
time (min)
190
170
150
130
110
90
70
50
30
10
-10
0
5
10
15
20
25
30
35
40

Figure 2.

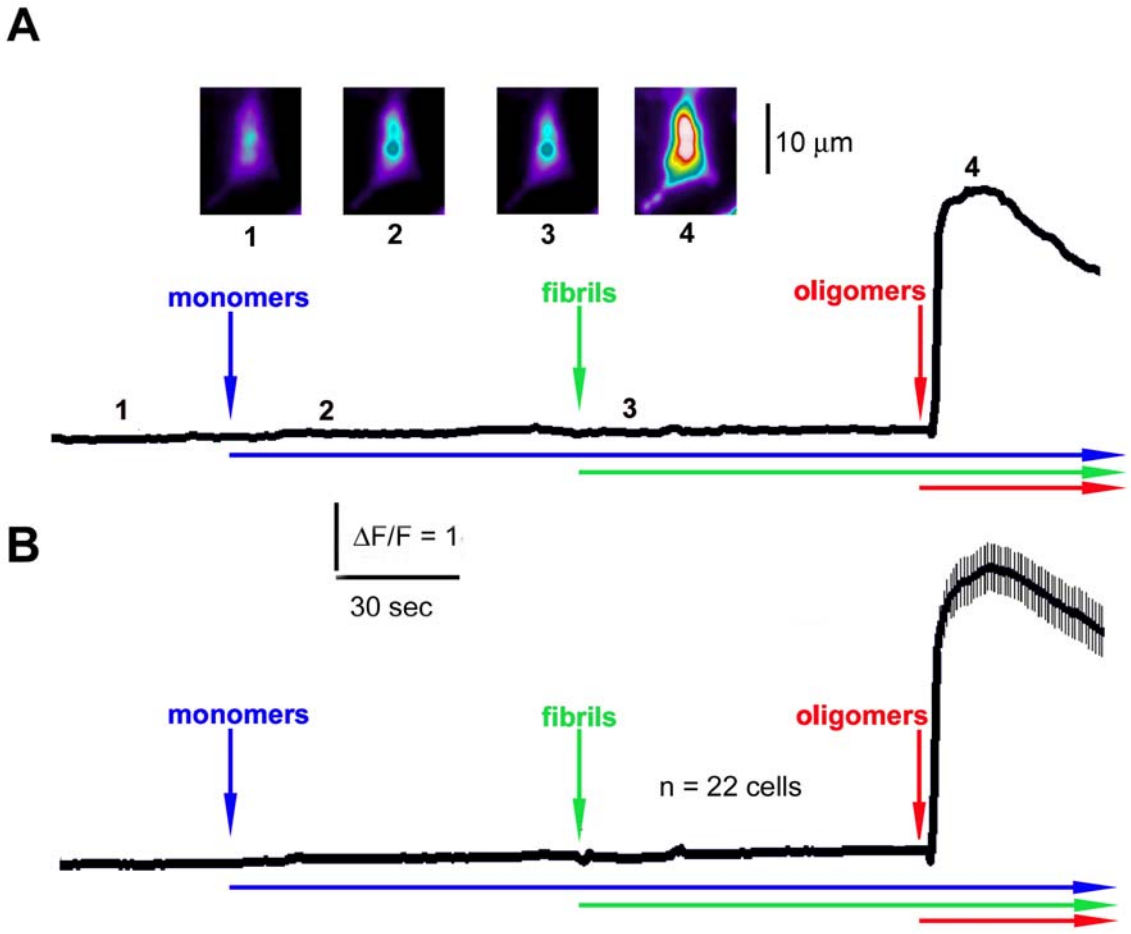
A
10 µm
1
2
3
4
monomers
fibrils
oligomers
1
2
3
4
B
ΔF/F = 1
30 sec
monomers
fibrils
oligomers
n = 22 cells

Figure 3.

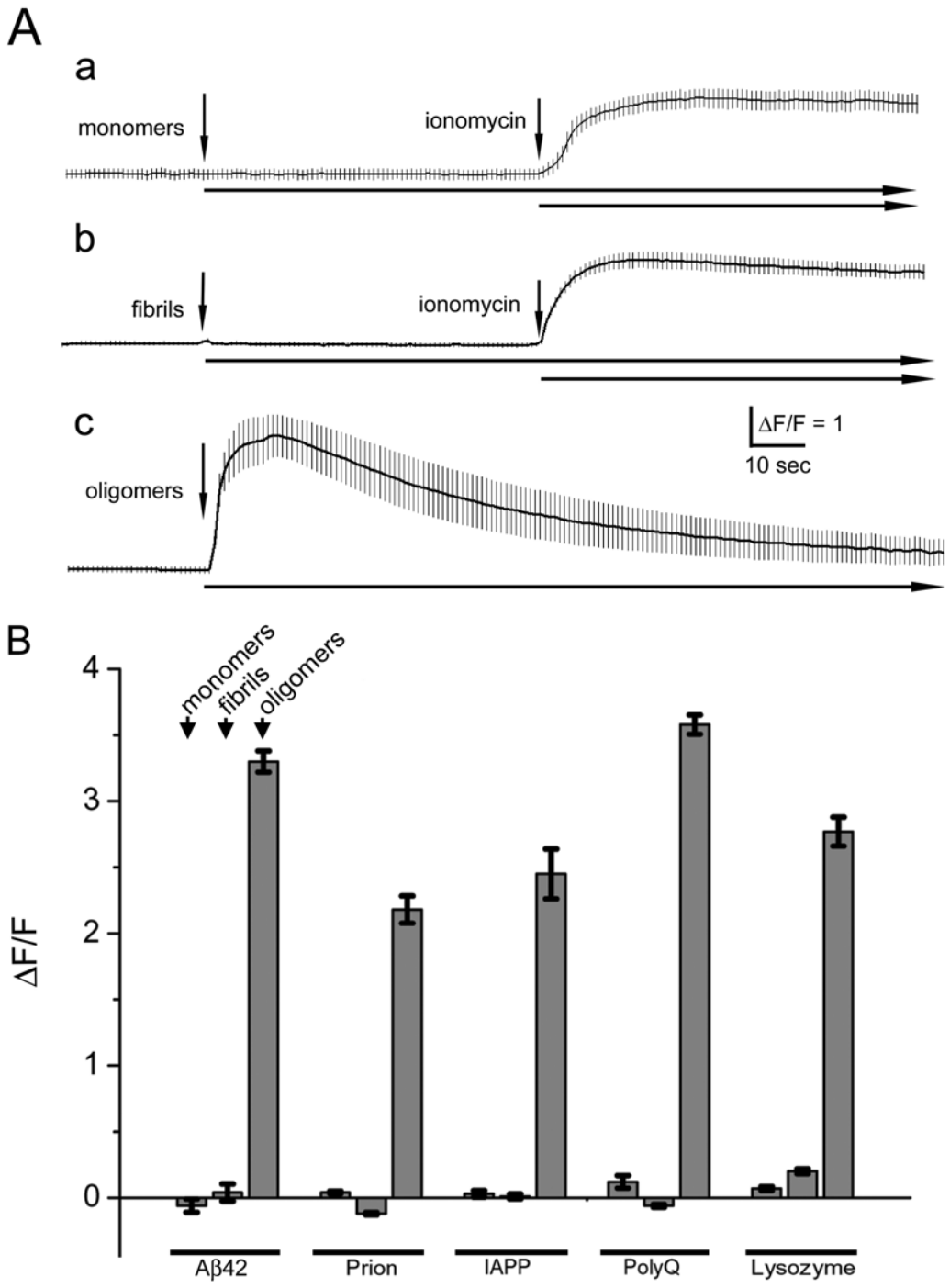
A
a
monomers
ionomycin
b
fibrils
ionomycin
c
oligomers
ΔF/F = 1
10 sec
B
monomers
fibrils
oligomers
ΔF/F
0
1
2
3
4
Aβ42
Prion
IAPP
PolyQ
Lysozyme

Figure 4.

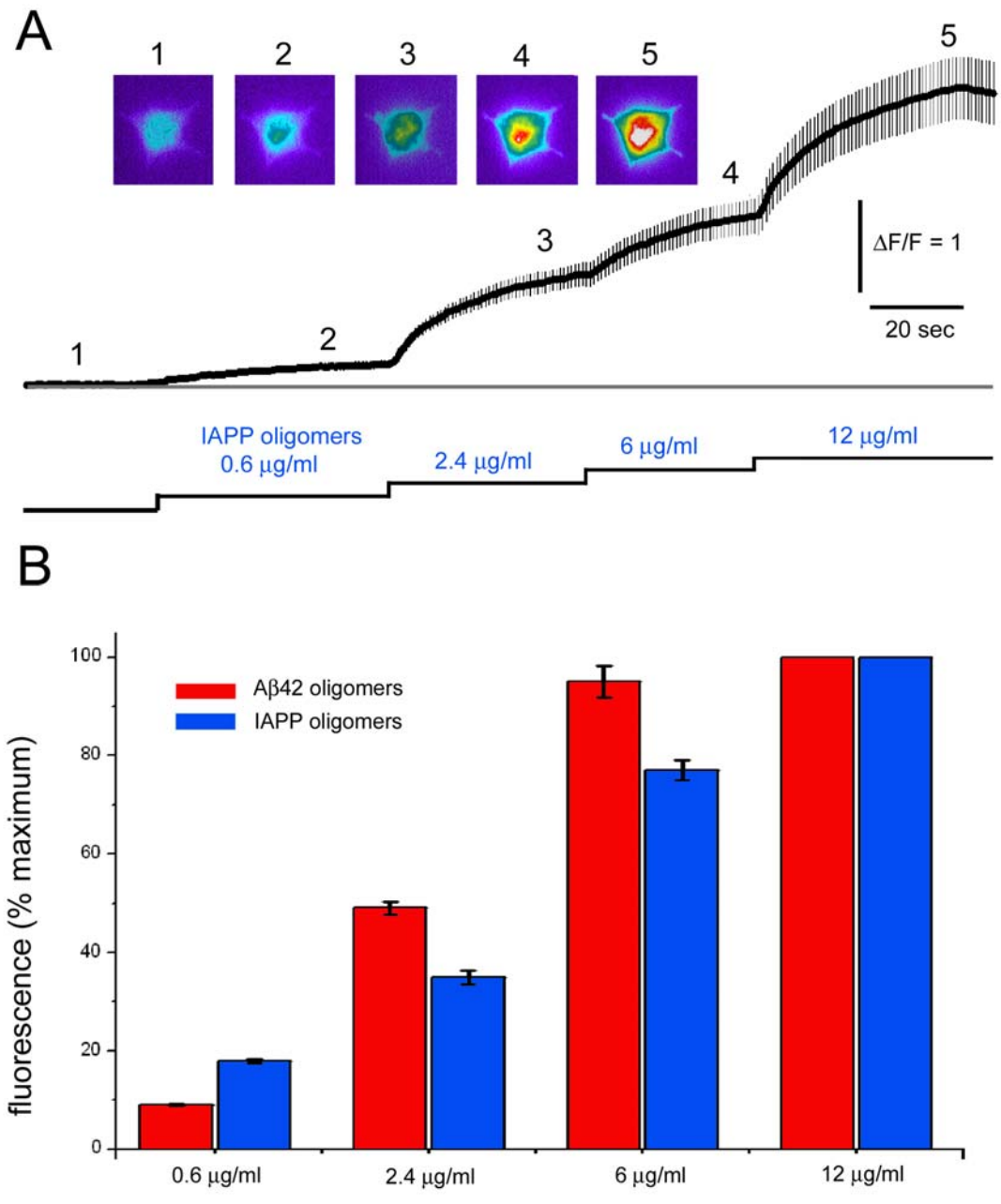
A
1
2
3
4
5
ΔF/F = 1
20 sec
IAPP oligomers
0.6 μg/ml
2.4 μg/ml
6 μg/ml
12 μg/ml
B
fluorescence (% maximum)
Aβ42 oligomers
IAPP oligomers
0.6 μg/ml
2.4 μg/ml
6 μg/ml
12 μg/ml

Figure 5.

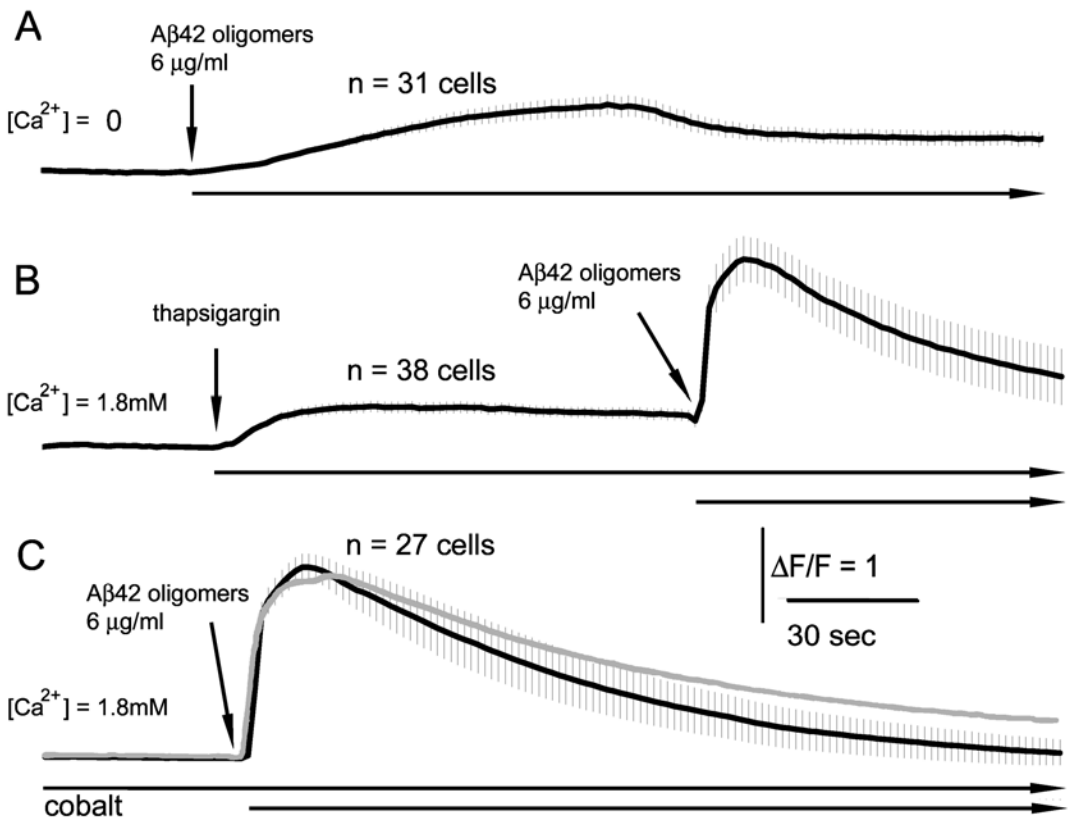
A
Aβ42 oligomers
6 μg/ml
n = 31 cells
[Ca2+] = 0
B
thapsigargin
Aβ42 oligomers
6 μg/ml
n = 38 cells
[Ca2+] = 1.8mM
C
n = 27 cells
ΔF/F = 1
30 sec
Aβ42 oligomers
6 μg/ml
[Ca2+] = 1.8mM
cobalt

Figure 6.

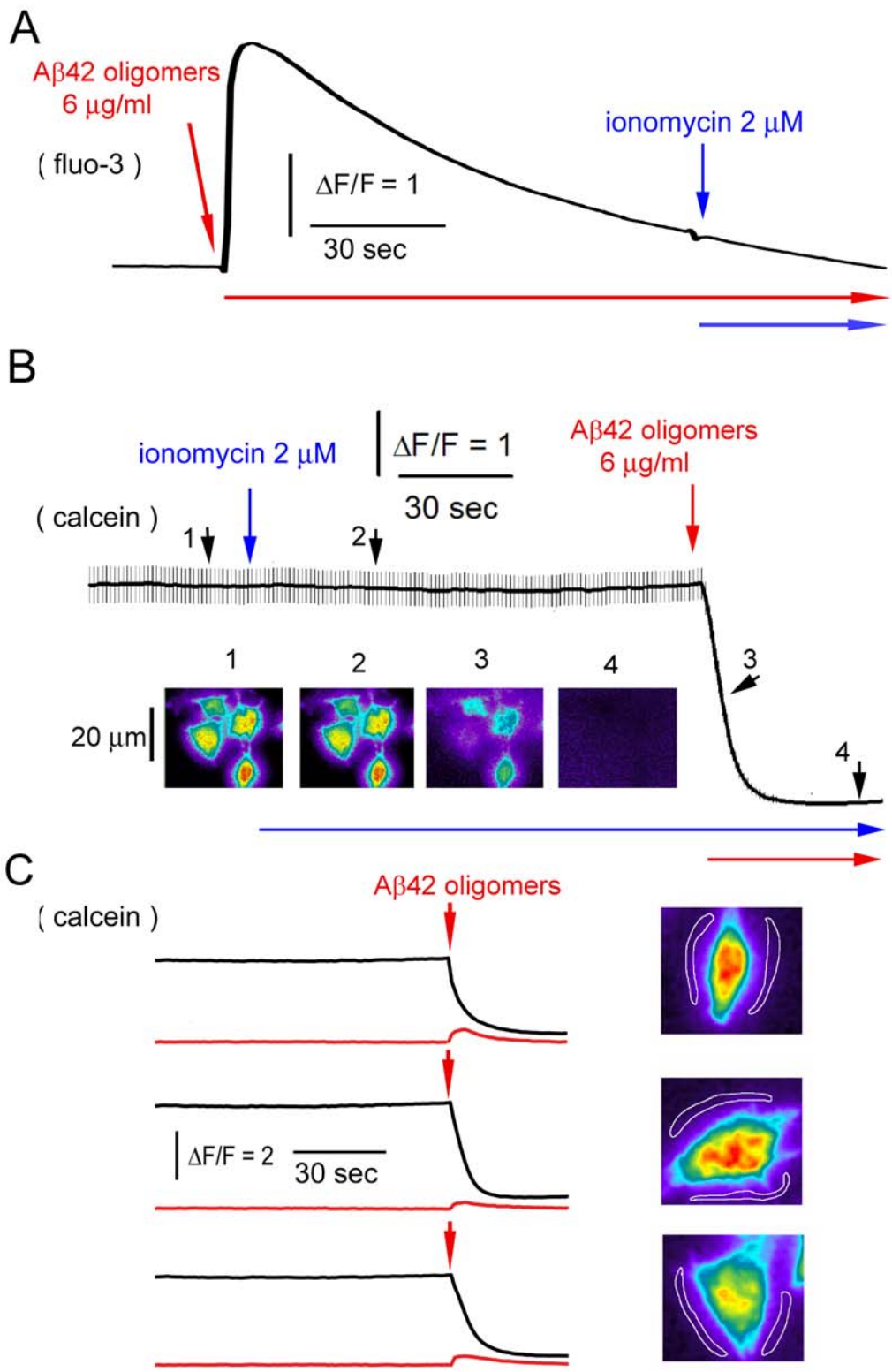
A
Aβ42 oligomers
6 μg/ml
(fluo-3)
ΔF/F = 1
30 sec
ionomycin 2 μM
B
ionomycin 2 μM
ΔF/F = 1
30 sec
Aβ42 oligomers
6 μg/ml
(calcein)
1
2
3
4
20 μm
C
Aβ42 oligomers
(calcein)
ΔF/F = 2
30 sec